Single Conjugated Adaptive **O**ptics **U**pgrade for **L**BT

SOUL-LUCI1 Performance

ID: SOUL-T06

Issue: 1.0

Released: September 18, 2020

Prepared by: Enrico Pinna, Cédric Plantet, Dino Mesa, Filippo Mannucci, Giuliana Fiorentino, Massimo Dall'Ora

INAF

Table of Contents

1 SCOPE OF THE DOCUMENT 2

2 INTRODUCTION 2

3 TOOLS FOR OBSERVERS 2

4 ON-AXIS PERFORMANCE 3

4.1 STREHL RATIO 3
4.2 FWHM 4
4.3 PSF AND CONTRAST 4
4.3.1 R5 - VERY BRIGHT 5
4.3.2 R8.6 - BIN 1 BRIGHT 6
4.3.3 R12.2 – BIN1 FAINT 7
4.3.4 R12.0 - BIN 2 BRIGHT 8
4.3.5 R13.5 - BIN 2 9
4.3.6 R 14.4 – BIN 3 10

5 OFF-AXIS PERFORMANCE 11

5.1 STREHL RATIO 11
5.1.1 SIMULATION 11
5.1.2 ON SKY (PALOMAR 10) 12
5.2 FWHM 15
5.2.1 SIMULATION 15
5.3 LIMITING MAGNITUDE (ETC CHECK) 16

6 EXAMPLES OF ASTROPHYSICAL OBSERVATIONS 17

6.1 LOW MASS COMPANION 17
6.1.1 2MASS J22362452+4751425 17
6.2 GLOBULAR CLUSTERS 19
6.2.1 M92 19
6.3 EXTRAGALACTIC 22
6.3.1 AGN J1630+1649 22
6.3.2 MORPHOLOGY OF DISTANT GALAXIES 22
6.3.3 DOUBLE STAR (FAKE EXTRAGALACTIC) 25

APPENDIX 1. WFS MAGNITUDE CALIBRATION 26

1 Scope of the document

This document provides an overview of the current performance of SOUL-LUCI1 at LBT to the observers that intend to use the instrument.

2 Introduction

SOUL is the upgrade of the FLAO and LBTI AO systems. Here we report about the upgrade of the FLAO system on the SX side of LBT, where it feeds the instrument LUCI1. The main goal of the upgrade is to allow AO operations with fainter guide stars, significantly improving the number of targets that can benefit of the turbulence correction, without the use of laser guide stars. SOUL-LUCI1 is pushing the boundaries of the previous limit on AO star brightness of about 1.5-2.0 magnitudes, and offering a wide pool of applications from high contrast on local object to high resolution in the extragalactic field. A wider description of the project and its main bibliography can be found on the webpage soul.arcetri.astro.it.

The SOUL-LUCI1 commissioning is in its final phase, but not yet completed. Here we report the performance characterization obtained so far. With the progress of the commissioning, this document will be updated and new issues released. As reported in the document, the system in its current status is already able to provide high quality data on a wide range of targets.

3 Tools for observers

Here is a list of list of the key tools for the observations with SOUL-LUCI1.

- **LUCI User Manual** (PDF on the LBTO webpage*)*
  SOUL-LUCI1 uses the N30 camera in imaging mode only; here you can find all the information about available filters and all camera features.

- **SOUL SR calculator** *(*web tool available on the *science with SOUL* webpage)
  this tool provides an estimation of the AO performance (Strehl ratio and PSF FWHM) for a set of input parameters (magnitude of the AO reference star, distance of the target, seeing, scientific wavelength). The performance values are based on numerical simulations that are compared to on sky measurement in this document.

- **LUCI Exposure Time Calculator** (web tool)
  select the *diffraction limited* option; insert in the *Strehl ratio* field the output obtained by the SOUL SR calculator (seeing value is not needed anymore in this step), magnitude and type (point or extended) of your target

- **LBTO Observing Tool** (SW tool, to be downloaded and installed)
  this is the tool for preparing the observation; follow the instructions reported in the linked webpage

- **Contact the project PI**: observers are welcome to contact the project PI for a preliminary evaluation of a possible targets (enrico.pinna@inaf.it)

4 On-axis performance

4.1 Strehl ratio

We report here (Figure 1) the Strehl Ratios (SR) measured on sky during the commissioning nights. The SR is measured on the AO reference star as imaged on LUCI1 N30 camera[1].

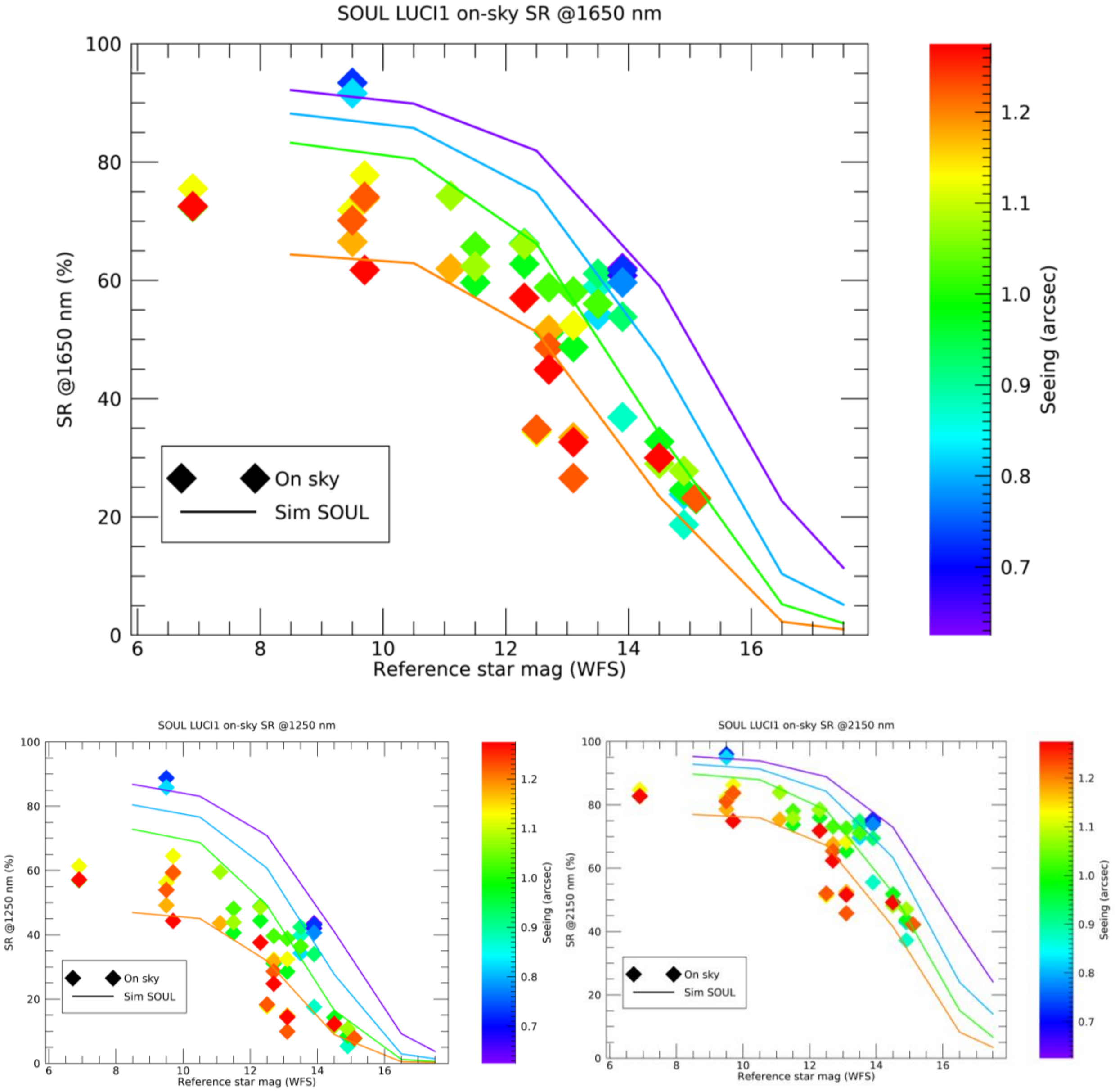

Figure 1. *Top*: on-sky SR in H (1650nm) as a function of WFS magnitude and seeing in the line of sight as measured by the DIMM (color code). The simulations results are plotted as solid lines for reference.
***Bottom*: same plot as above, rescaled to J (left) and K (bright) bands.**

The on-sky SRs (diamonds) are compared with the simulation results (lines) and the color indicates the seeing in the line of sight. To produce this figure, we used a data set of 151 observations sorted in magnitude bins of 0.2 and seeing bins of 0.05” (56 bins in total). Each point of the figure corresponds to the

[1] Most of the SRs have been measured with FeII or H filters and a few in H2 or Ks ones and then rescaled using Marchal’s approximation. Each SR measurement is performed on a total exposure time from a few to tens of seconds just averaging the sub-frames, without any shift & add or frame selection process. The use of these technique can significantly improve the SR values.

average SR in the corresponding 2D bin (magnitude/seeing). The simulation curves include an average amount of telescope vibrations and correspond to the values available on the SOUL SR calculator. These can vary significantly with wind (strength and direction) and dome environment (instrumentation like pumps etc). We have quite a good agreement between on sky measurement and simulations. Above 60% at 1650nm we observe a higher dispersion attributed to the NCPA[2], not compensated in most of the cases. On sky results are missing on the very faint end (WFS mag> 15), as we are still optimizing the system for low fluxes. It is important to note that the magnitude shown here (WFS mag) is the one computed on the flux measured by the SOUL WaveFront Sensor (WFS). As we will detail in Appendix 1, this magnitude can be approximated as R magnitude[3] for an M3 type star and R-0.9 for a G2V one.

4.2 FWHM

In Figure 2 we report the measured FWHM[4] on the AO reference star using the same dataset and bin process as in 4.1, but limiting the sample to data measured with H or FeII filters. The on sky values show a good agreement with simulations.

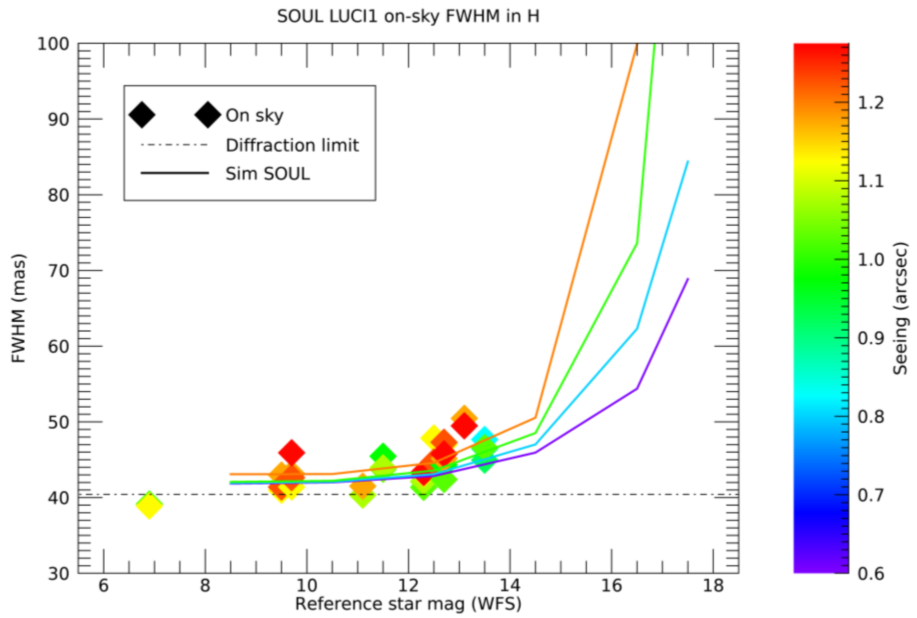

Figure 2. FWHM of the AO reference star measured on sky on LUCI1 in H band (or FeII) as function of the reference star mag and seeing (color code). Dashed line represents the diffraction limit. Solid lines are the values obtained via numerical simulation with average vibrations.

4.3 PSF and contrast

In this section, we report a selection of PSF images and contrast curves measured on AO reference stars at different magnitudes: from R5 (very bright end) down to R14.4 (this is not the working limit of the system, just where this collection stops). The SOUL system demonstrates here to deliver a remarkable level of correction even with reference star fainter than R12, when typically NGS SCAO systems drop their performance more drastically. No NCPA correction has been applied; low order static aberrations are present and may impact mainly on the higher SR values and on the shape of the first diffraction ring.

[2] NCPA stands for Non Common Path Aberrations. NCPA can be partially compensated by the AO system, but this compensation is not still available for routine observations.
[3] Where not differently specified, in this document we refer to Vega magnitudes.
[4] The value is obtained with a fit of Moffat function and then averaging major and minor axis FWHMs. The Moffat fit, for high SR values can introduce an underestimation of the FWHM of a few %. This explains the values under the diffraction limit obtained for mag ~7.

4.3.1 R5 - Very bright

This star has been observed using the sub-windowing of LUCI with 256x256 frames allowing to reduce the DIT down to 0.3s. Even reducing the DIT, the star peak was saturating the detector. The peak flux has been measured using a neutral density (ND2) in LUCI. This allowed the measurement of main peak and first ring fluxes, used to recover the correct scaling of the contrast in the saturated image.

AO Parameters	Value
AO reference star	V 5.8 - **R 5.4** - J 4.7
Seeing (DIMM Line of sight)	0.9"-1.3" (07Jul2020)
# of corrected modes	500
AO loop frequency	1700 Hz
WFS binning	1x1 (40x40SA)
Strehl ratio	73% (FeII+ND) 82% (H2 + ND)

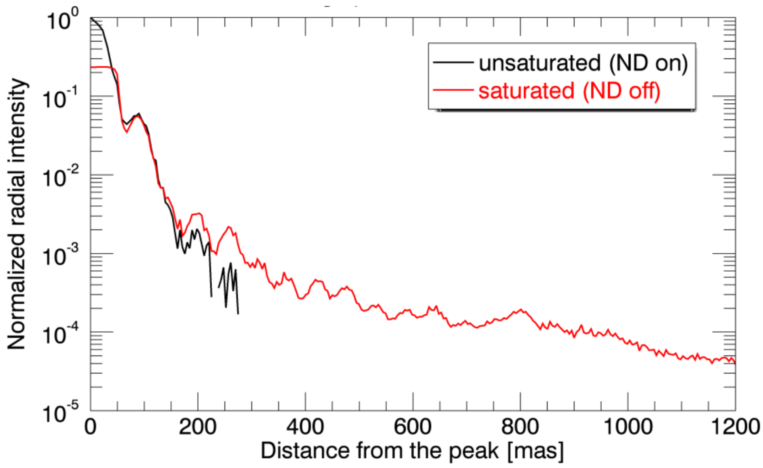

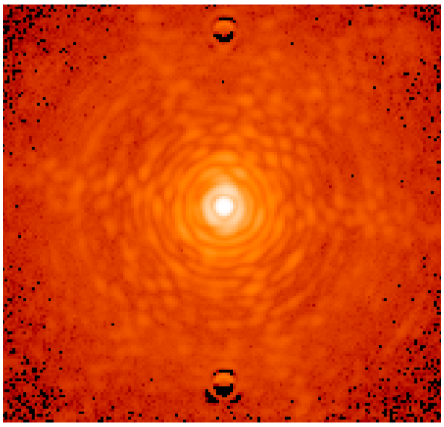

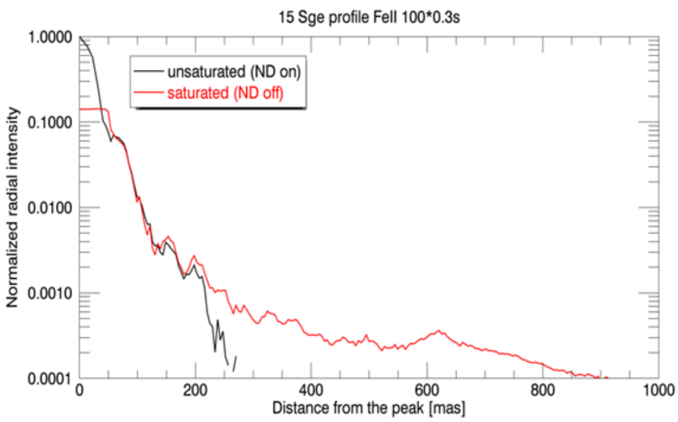

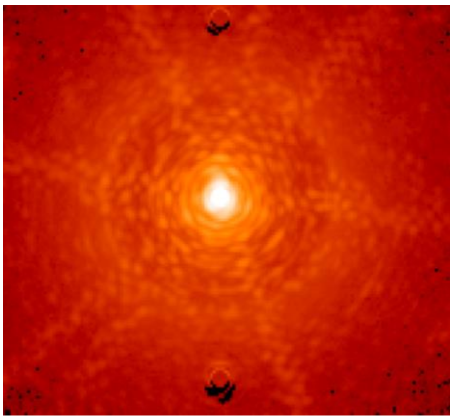

Figure 3. ***Left*: intensity radial profiles for H2 and FeII filters, top and bottom respectively.**
***Right*: the corresponding frames displayed in log-scale.**

4.3.2 R8.6 - Bin 1 bright

AO Parameters	Value
AO reference star	B 10.3 - V 9.3 - **R 8.6** Sp. T. = K3
Seeing (DIMM Line of sight)	0.7"-0.8" (01Nov2018)
# of corrected modes	500
AO loop frequency	1700 Hz
WFS binning	1x1 (40x40SA)
Strehl ratio (2150nm)	80%

-

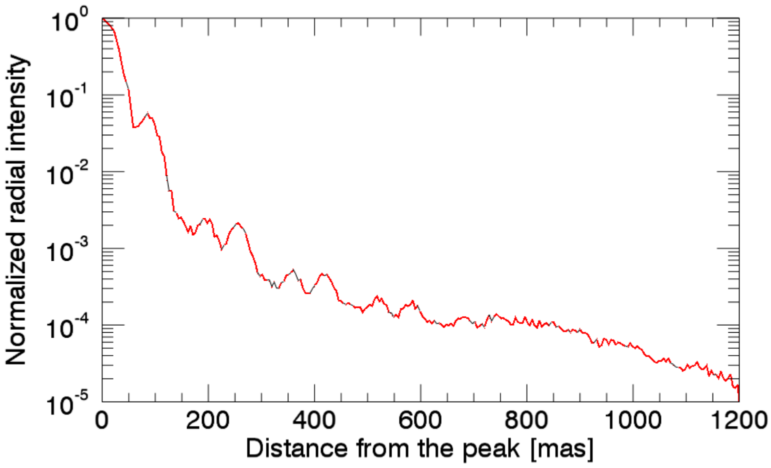

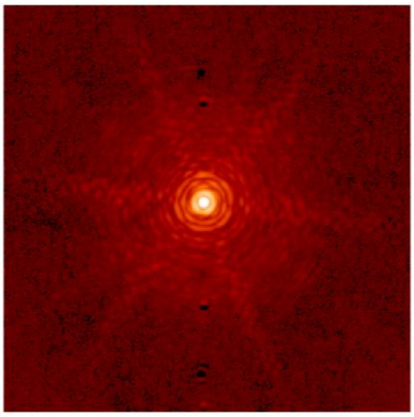

Figure 4. H2 filter (2150nm), sum of 60 frames of 0.3s exposure each.
***Left*: intensity radial profile, normalized to the peak.**
***Right*: frame displayed in log-scale with side 3.84".**

4.3.3 R12.2 – Bin1 Faint

AO Parameters	Value
AO reference star	V 12.3 - **R 12.2** Sp. T. K5 D
Seeing (DIMM line of sight)	1.1” (01Nov2018)
# of corrected modes	500
AO loop frequency	401 Hz
WFS binning	1x1 (40x40 SA)
Strehl ratio (2150nm)	80%

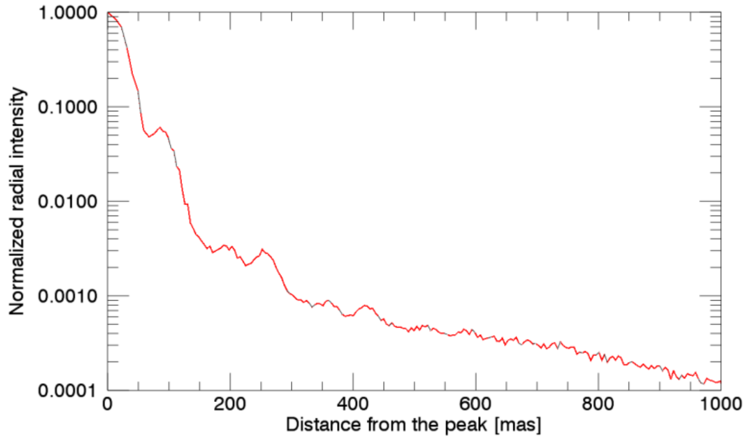

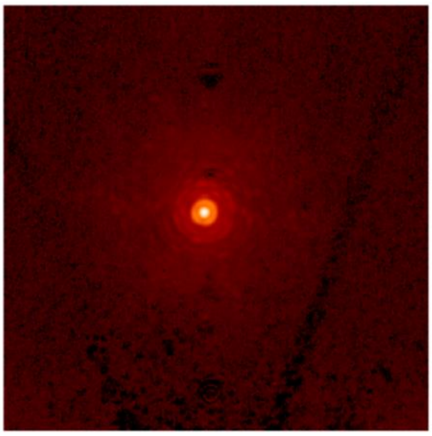

Figure 5. Filter H2(2150nm), sum of 15 frames of 3.0s exposure each.
Left: **intensity radial profile, normalized to the peak.**
Right**: frame displayed in log-scale with side 3.84”.**

4.3.4 R12.0 - Bin 2 bright

R12 results on the edge for bin1 and bin2 configuration. The configuration is selected automatically by the AO system based on the flux recorded on the WFS. This star was providing a slightly smaller flux w.r.t. to the previous one, even if the catalogue was reporting a brighter value in R. This resulted in having the system to select Bin2 instead of Bin1 configuration, correcting a lower number of modes, but at higher frequency for a better vibration rejection.

AO Parameters	Value
AO reference star	V 12.8 -**R 12.0**
Seeing (DIMM Line of sight)	0.9”-0.11” (03Jul2020)
# of corrected modes	250
AO loop frequency	1200 Hz
WFS binning	2x2 (20x20 SA)

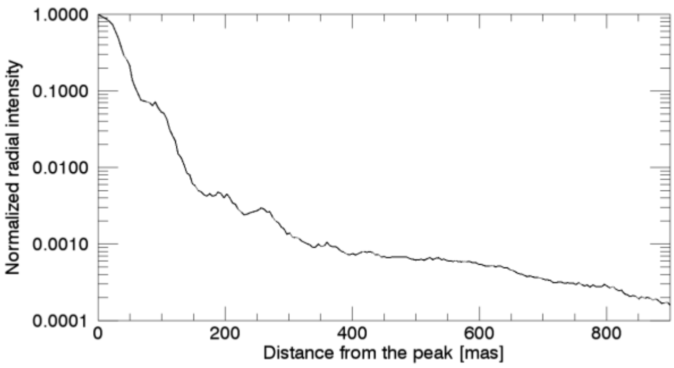

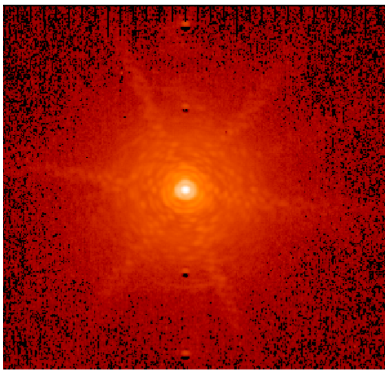

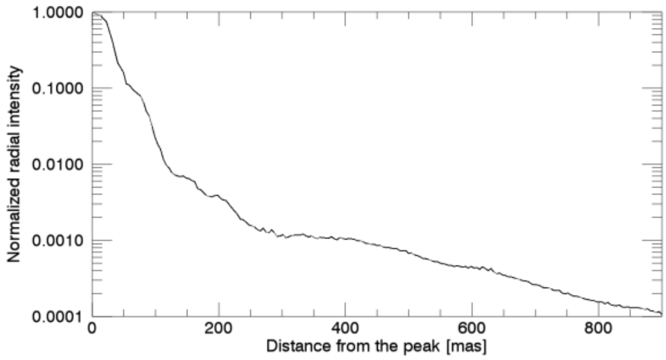

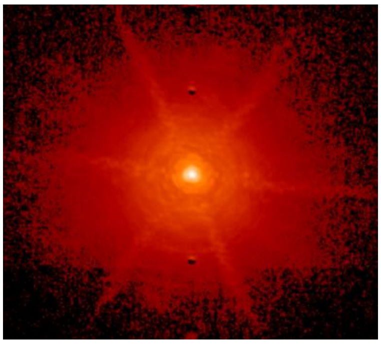

Figure 6 *Top*: H2 (2150nm) Intensity radial profile (left) and log display of the frame (right).
Bottom: FeII (1650nm) Intensity radial profile (left) and log display of the frame (right).

4.3.5 R13.5 - Bin 2

AO Parameters	Value
AO reference star	B 15.7 - **R 13.50** Sp. T: M3 D
Seeing (DIMM Line of sight)	0.9” (09Jul2019)
# of corrected modes	250
AO loop frequency	870 Hz
WFS binning	2x2 (20x20 SA)
Strehl ratio (1650nm)	63%

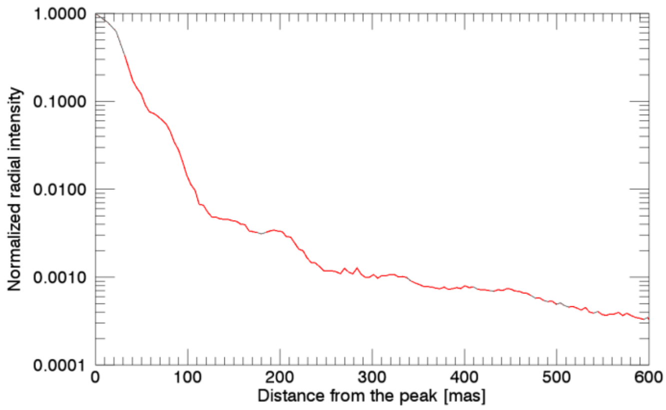

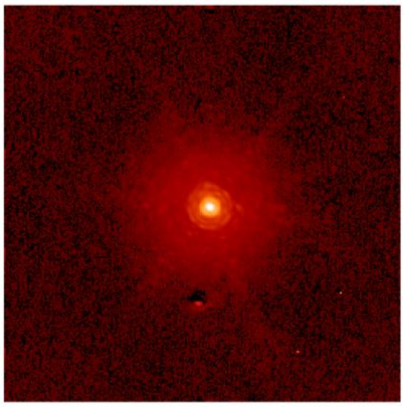

Figure 7. Filter FeII (1646nm), sum of 40 frames of 2.0s exposure each.
Left: **intensity radial profile, normalized to the peak.**
Right**: frame displayed in log-scale with side 3.84”.**

4.3.6 R 14.4 – Bin 3

AO Parameters	Value
AO reference star	B 14.3 - V 14.0 - **R 14.4**
Seeing (DIMM Line of sight)	1.0" (09Jul2019)
# of corrected modes	250
AO loop frequency	870 Hz
WFS binning	3x3 (13x13 SA)
Strehl ratio (2150nm)	47%

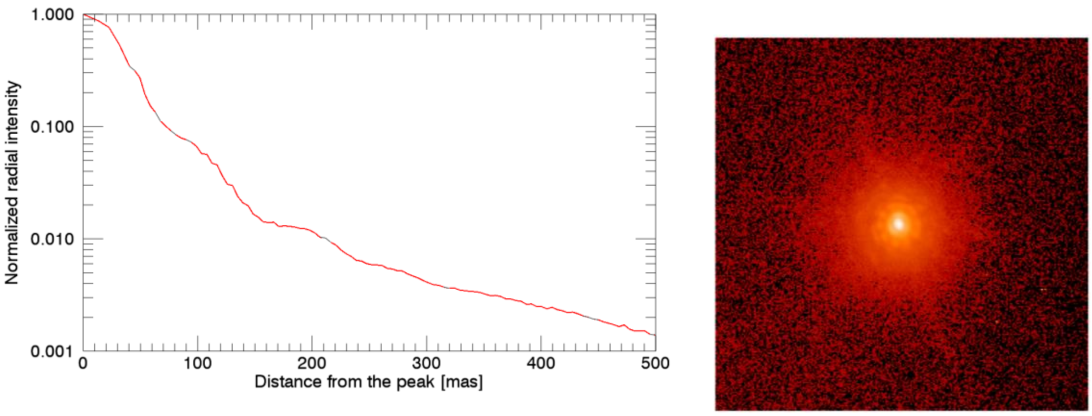

Figure 8. Filter Ks (2150nm), sum of 10 frames of 10s exposure each.
***Left*: intensity radial profile, normalized to the peak.**
***Right*: frame displayed in log-scale with side 3.84".**

5 Off-axis performance

SOUL is a SCAO system, so it is able to provide active correction of the turbulence on the AO reference direction only. Objects that are off-axis will only partially benefit from this correction. The quality of the off-axis correction is determined by the on-axis correction combined with the vertical distribution of the atmospheric turbulence. This distribution can vary for the same seeing value leading to very different results.

In this section, we will report performance expected by numerical **simulations** obtained considering **one single case of vertical distribution** assumed as a median case. These values are a subset of those feeding the SOUL SR calculator. Then, in 5.1.2 we compare simulated SR values with on sky data of a globular cluster.

5.1 Strehl ratio

5.1.1 Simulation

Here we report the SR foreseen as function of the distance from the AO reference star for K and J bands considering seeing of 1.0” and one particular case of turbulence vertical distribution[5].

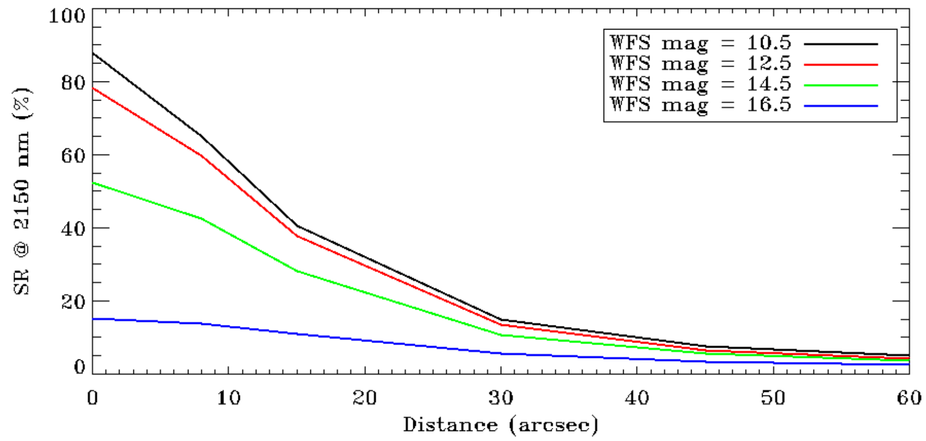

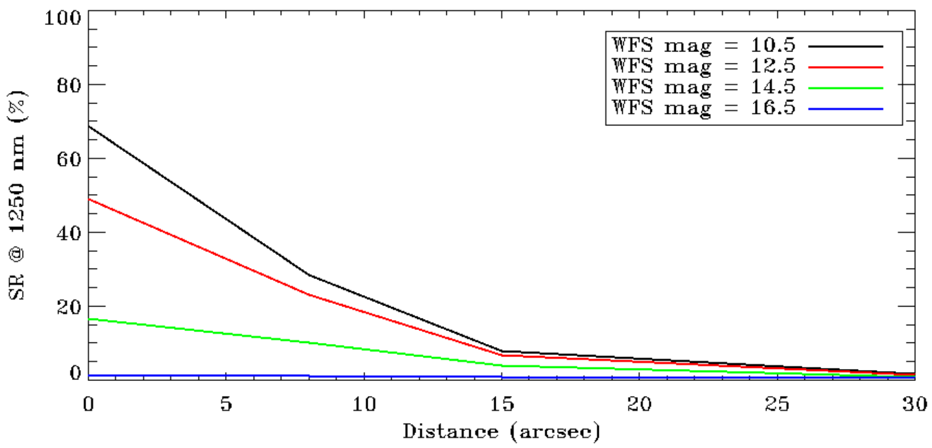

Figure 9. SR values off-axis as expected by simulation with seeing 1.0” and the considered case of turbulence vertical distribution

[5]Tthe considered profile is the typical one for LBT reported in “Optical turbulence vertical distribution with standard and high resolution at Mt. Graham” - 2010 Masciadri et al., while the considered median wind is from “Wind speed vertical distribution at Mt Graham” – 2010 Haglin et al.

and a sample of 4 AO star brightness in K band (top) and J (bottom).

5.1.2 On sky (Palomar 10)

We report here two observations of the same field of globular cluster Palomar 10 done on June 23rd and July 3rd 2020 both in J and Ks bands. We selected a sample of 30 stars spread in the field and we computed the SR for each of them. The seeing measured by the DIMM was similar in both observations (between 0.9" and 1.1", slightly worse on July 3rd). The analysis shows here that the correction across the field was quite different (see Figure 11) due to a different vertical distribution of the turbulence power. In the plots we compare the measured SRs with those foreseen by simulations for 3 different values of seeing, but just one vertical distribution. Ks and J plots both show that the vertical distribution on the July 3rd is close to the one considered in simulations, while the one on June 23rd shows a more favorable distribution with a slower degradation of performance with distance from AO reference.

AO Parameters	Value
AO reference star	B 13.9 - V 13.1 - **R 12.1**
Distance from the target	0-40"
Seeing (DIMM Line of sight)	0.8"-1.1" (Jun 23, 2020) 0.9"-1.3" (Jul 03, 2020)
# of corrected modes	250
AO loop frequency	900 Hz
WFS binning	2x2 (20x20 SA)

5.1.2.1 Ks filter

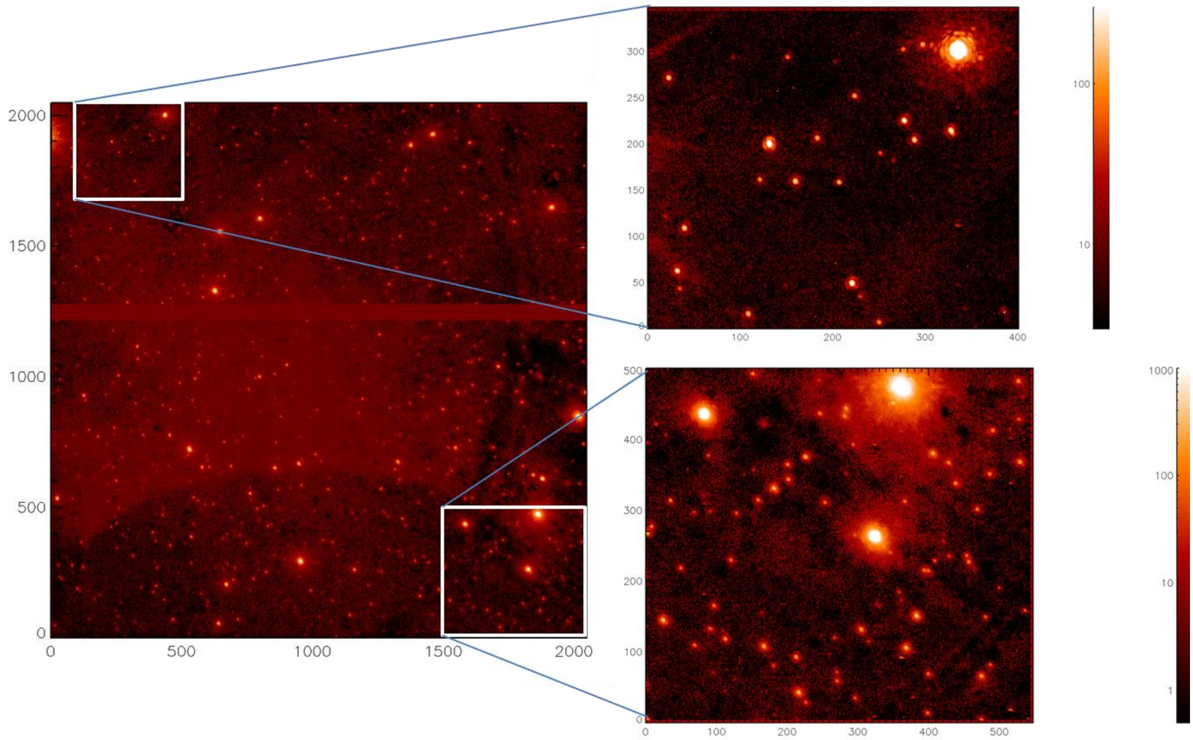

Figure 10. Display in log-scale of one dithering position (3min exposure) of Palomar 10 in Ks-band, acquired on June 23rd 2020. The insets show the detail of the single star images close and far from the AO ref star. The X and Y units are camera pixel with

platescale 0.015"/pix.

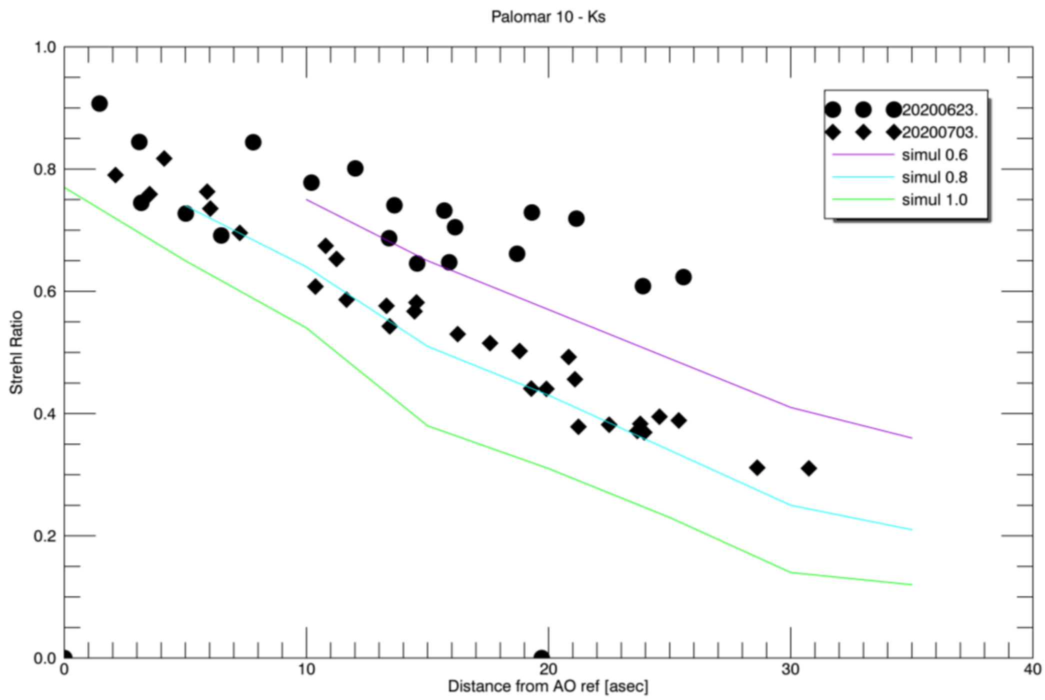

Figure 11. SR value in Ks-band computed on the sample of 30 stars and plotted as function of their distance from the AO reference star. We report the values on the same stars for 2 different observations of the same field. Solid lines report the simulation for 3 different seeing values.

5.1.2.2 J filter

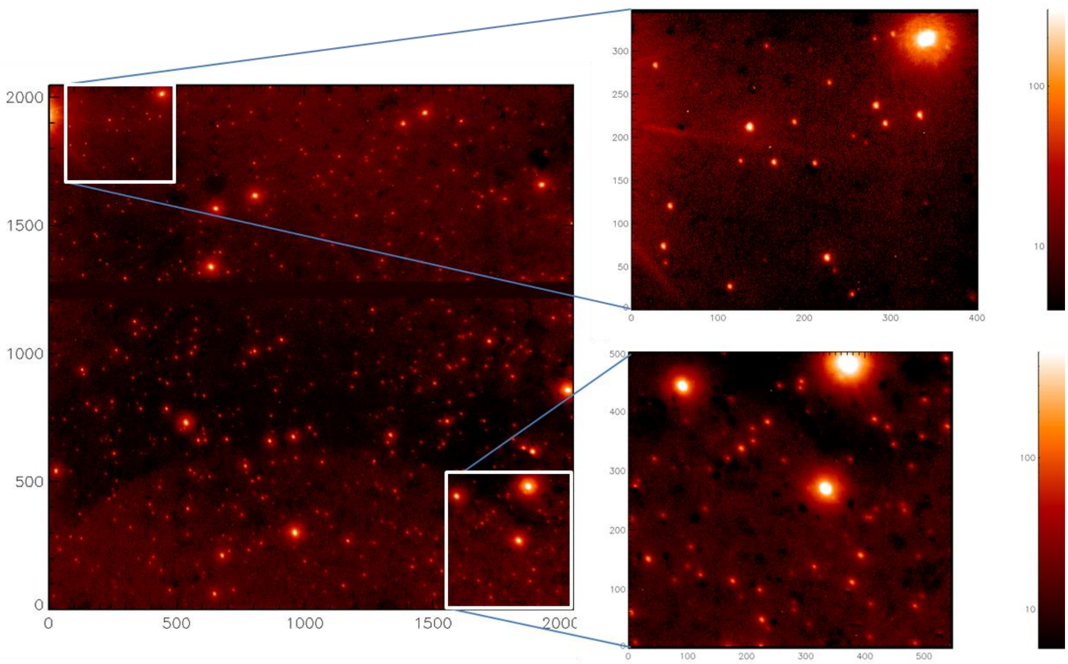

Figure 12. Display in log-scale of one dithering position (3min exposure) of Palomar 10 in J-band, acquired on June 23rd 2020. The insets show the detail of the single star images close and far from the AO ref star.

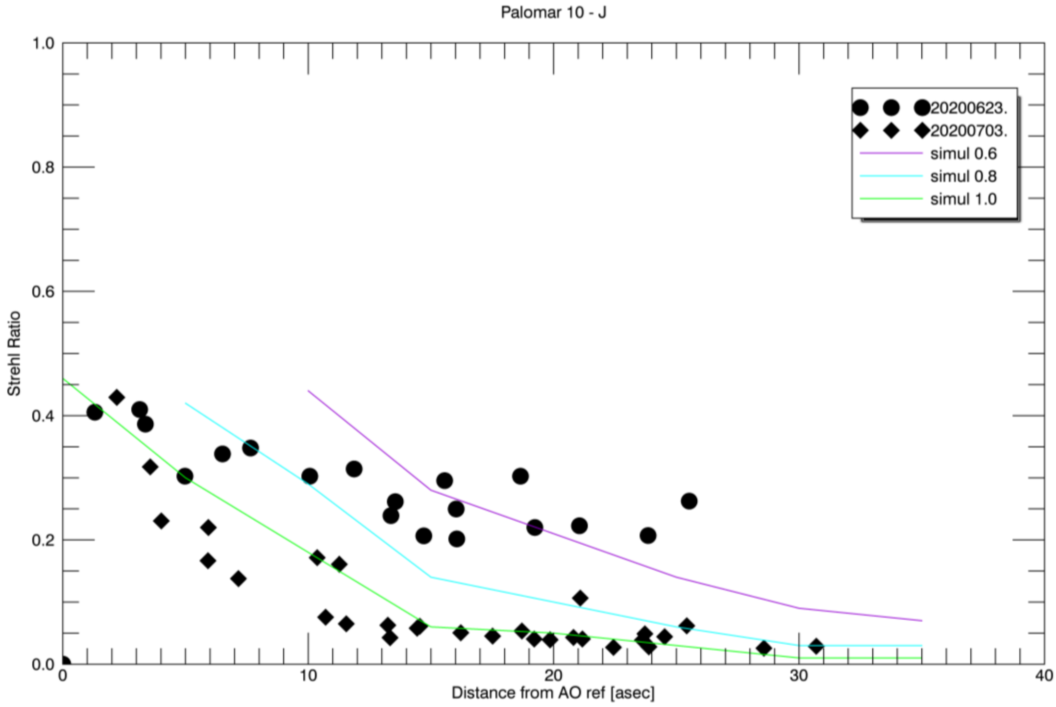

Figure 13. SR value in J-band computed on the sample of 30 stars and plotted as function of their distance from the AO reference star. We report the values on the same stars for 2 different observations of the same field. Solid lines report the simulation for 3 different seeing values.

5.2 FWHM

5.2.1 Simulation

In we report the FWHM[6] foreseen as function of the distance from the AO reference star for K and J bands considering seeing of 1.0" and one particular case of turbulence vertical distribution.

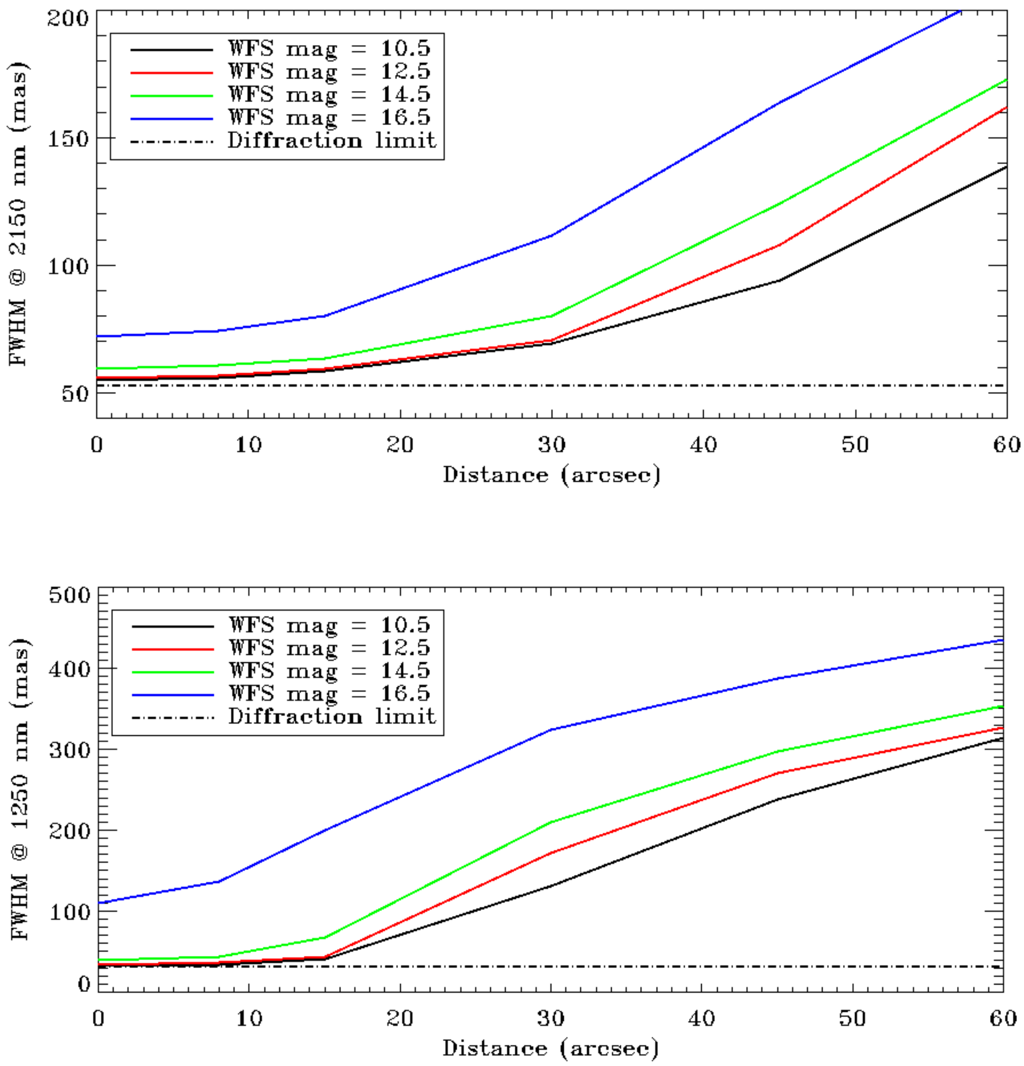

Figure 14. PSF FWHM off-axis as expected by simulation with seeing 1.0" and the considered case of turbulence vertical distribution. The values in K (top) and J-band (bottom) are plotted as function of the distance from the AO reference star for a sample of 4 magnitudes.

[6]For simulation we compute the FWHM value as radial average on the PSF highly sampled.

5.3 Limiting magnitude (ETC check)

From the observations performed in M92 and described in 6.2.1, we derived the following limiting magnitudes:

J-band (6x3 sec) ~ 20.5 mag - SN ~7
J-band(180 sec) ~23 mag - SN ~2

K-band (6x3 sec) ~ 19.5 mag - SN ~5
K-band(180 sec) ~ 21 mag. - SN ~2

Here below, we report the Luci1 ETC calculator expected values, considering source temperature 3000K and SR of 0.4 and 0.7[7] for J and Ks respectively.

SN (J =20.5 mag - 54s) ~ 12
SN (J =23 mag - 180s) ~ 4

SN (K =19.5 mag - 54s) ~ 20
SN (K =21 mag - 180s) ~ 9

The measured SN values are in good agreement with the ETC ones in J band, while SN measured is K band is lower than expected. We attribute this discrepancy to the lack of focal plane mask during the observation, as mentioned in section 6.

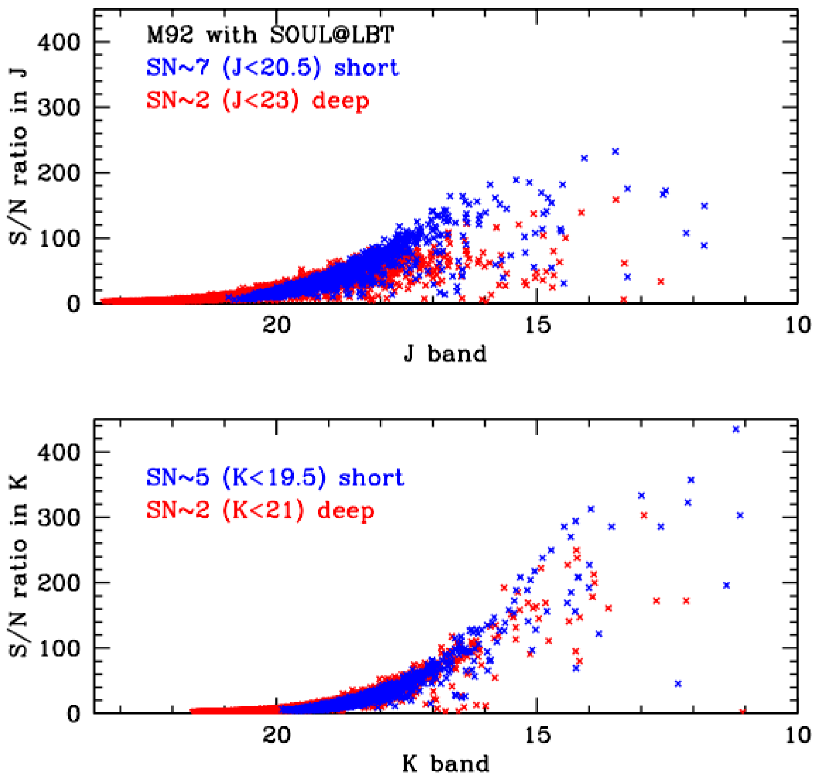

Figure 15. SN ratio of the short (blue) and long (red) exposures in J (top) and K (bottom) bands. The detected limiting magnitude and their SN are also reported.

[7] We considered these SR values as the expected ones at a distance of 10 asec from the AO reference star.

6 Examples of astrophysical observations

Here we report about a few short (about 1h or less) observations carried out during the commissioning nights, mainly but not only in June-July 2020. The observations have been performed running the observing blocks prepared by the astronomer with the support of an astronomer and using the LBT "Observing tool".

During the run of June-July 2020, the focal plane mask in LUCI1, limiting the field to 30"x30", was not available due to a temporary failure. The missing mask produces intensity patterns that are not completely corrected by the sky subtraction. This resulted in some residual gradient and pattern in the frame (see Figure 10). Moreover, one of the read-out channels of LUCI1 was not working making one stripe of 63x2048 pixels unavailable (see again Figure 10). Currently, the LUCI1 read-out and mask exchanger are both back to its full functionality.

6.1 Low mass companion

6.1.1 2MASS J22362452+4751425

To test the capabilities of the instrument in the imaging of sub-stellar companions of main sequence stars we observed the late-K spectral type star 2MASS J22362452+4751425 belonging to the AB Doradus moving group with an estimated age of ~120 Myr. A sub-stellar companion was discovered at a separation of 3.7" (corresponding to around 230 au) was discovered by Bowler et al. 2017 using NIRC2 adaptive optics at Keck telescope. They estimated for this object a mass of 11-14 M_{jup} at the limit between planets and brown dwarfs.

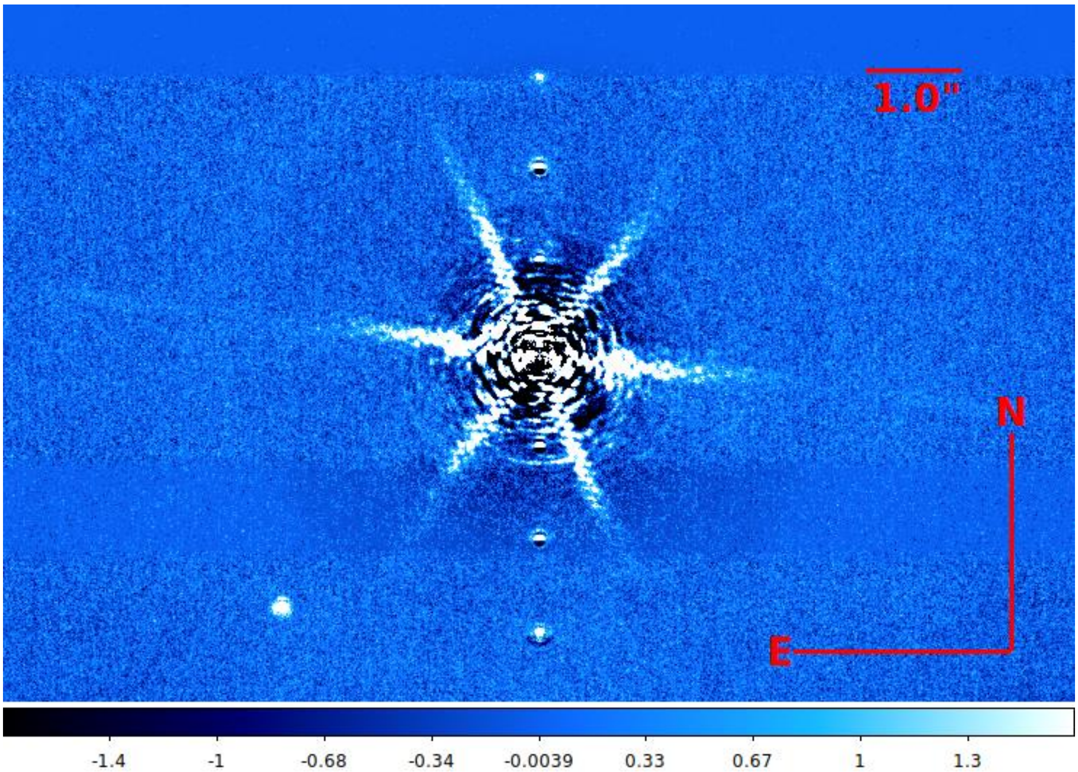

Figure 16. Final image obtained for 2MASS J22362452+4751425 using the H2 filter. The sub-stellar companion is clearly visible South-East of the star.

Table 1. Astrometric and photometric values obtained for 2MASS J22362452+4751425 b for both the filters in our data.

Filter	Δα (mas)	Δdec (mas)	Separation (mas)	PA (°)	Contrast	Contrast (mag)
H2	2658.00	-2614.50	3728.35	134.53	5.81×10^{-4}	8.09
FeII	2661.00	-2614.50	3730.49	134.50	2.95×10^{-4}	8.83

The target was observed in the night of 2020-07-03 in good weather conditions and seeing 0.9”-1.0”. The target was observed both in the H2 and the FeII filter. To simplify the observing sequence we did not apply any rotation during it so that it was not possible to apply any high-contrast imaging technique (e.g. angular differential imaging) to these data. The observations were carried on applying dithering with the star in different positions of the detector to be able to build a bias (through a median on the full dataset) to be subtracted from each raw frame. The reduced data were then recentered and combined applying a median on the dataset. We also subtracted PSF profile from each image to improve the quality of the final image. The final result of this procedure is shown in Figure 16, where the companion is clearly visible South-East from the star. A similar final image was obtained for the FeII filter (not shown here). We were also able to obtain reliable astrometric and photometric values for the filters. We listed all them in Table 1. Finally, we were also able to calculate the contrast for our observations. As an example we show in Figure 17 the final contrast obtained for the H2 filter. In this Figure, we show both the plot obtained simply applying a median of the full dataset (solid line) and subtracting the PSF profile from each image (dashed line). As a comparison, we also plot the position of the sub-stellar companion that is indicated by a blue square.

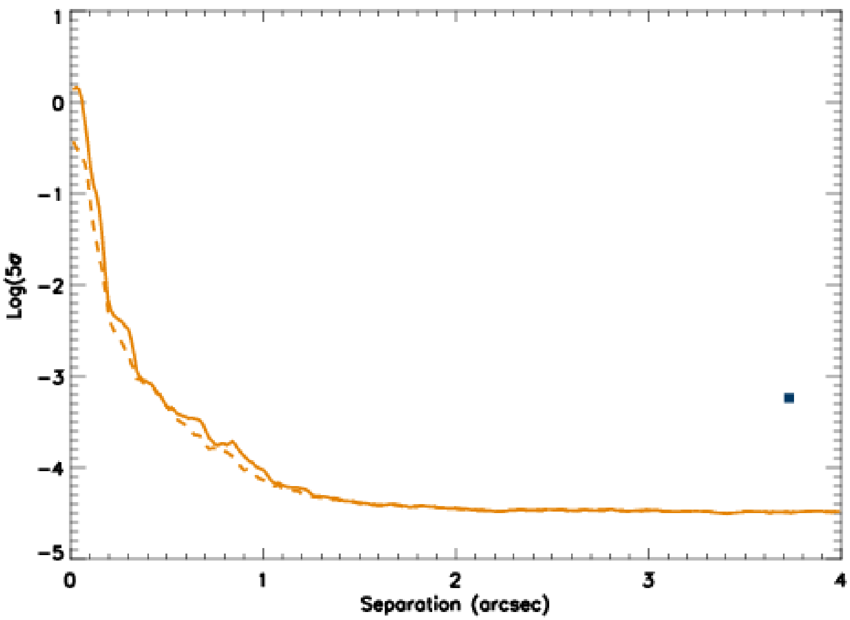

Figure 17. Final contrast obtained for 2 MASS J22362452+4751425 using the H2 filter. The solid line is obtained using the median of the dataset while the dashed line is obtained subtracting the PSF profile from the images.

6.2 Globular clusters

6.2.1 M92

With the goal to test SOUL performance, we have selected a well-known globular cluster for which deep Near Infrared photometry does not exist. As a scientific goal, we want to reach deeper J and K magnitudes in order to detect the main sequence knee. To do so, we have planned deep J and Ks observations, i.e. 6 images of 180 second each in both bands. We have also included short observation to recover the brighter part of the colour-magnitude-diagram (CMD), i.e. 6 images of 3 seconds each in both bands, this help in both better constrain the Main Sequence Turn off (a crucial anchor for the MSK) and in calibration purpose.

At a first glance of the data, the quality seems very good. The DIMM seeing was quite stable and good (0.6”-0.8”) during our observations. In order to test it, we have performed a preliminary, standard (Daophot/Allstar, Stetson 1994), photometric analysis of the dull set of short images and of one J and one Ks deep images to check the quality of the data. This is a preliminary photometry since as first step we have used a costant PSF across the FoV, in the following we will fine tune the analysis for SOUL AO images that include a, although slight, PSF variation (see Figure 18 and Figure 19).

AO Parameters	Value
AO reference star	V 11.8 - **R 11.4 -** I 10.8
Distance from the target	0-20’’
Seeing (DIMM Line of sight)	0.6”-0.8” (Jun 23)
# of corrected modes	500
AO loop frequency	625 Hz
WFS binning	1x1 (40x40SA)

The results are shown in Figure 20 and Figure 21 for J and K band respectively. We have preliminary calibrated our data, by applying a rigid shift to match magnitude and colours of theory and observation. We have selected a theoretical alpha-enhanced (+0.4) isochrone with metallicity [Fe/H]~ -2.3 and age of 13 Gyr. We have adopted a visual distance modulus of muV=14.74 and E(B-V)=0.023, accordingly to the recent analysis of deep HST data discussed in VandenBergh et al. 2016 (2016ApJ...827....2V). This rough calibration is compatible with the shallow near infrared photometry provided by Lee et al. 2001 (2001AJ....122.3136L) and del Principe et al. 2005 (2005AJ....129.2714D).

Concluding we do expect to improve our photometry by fine tuning the PSF-analysis and we are very confident to reach with the right S/N ratio the MSK feature which is located at 19.6 mag and 20.6 mag in K and J band respectively.

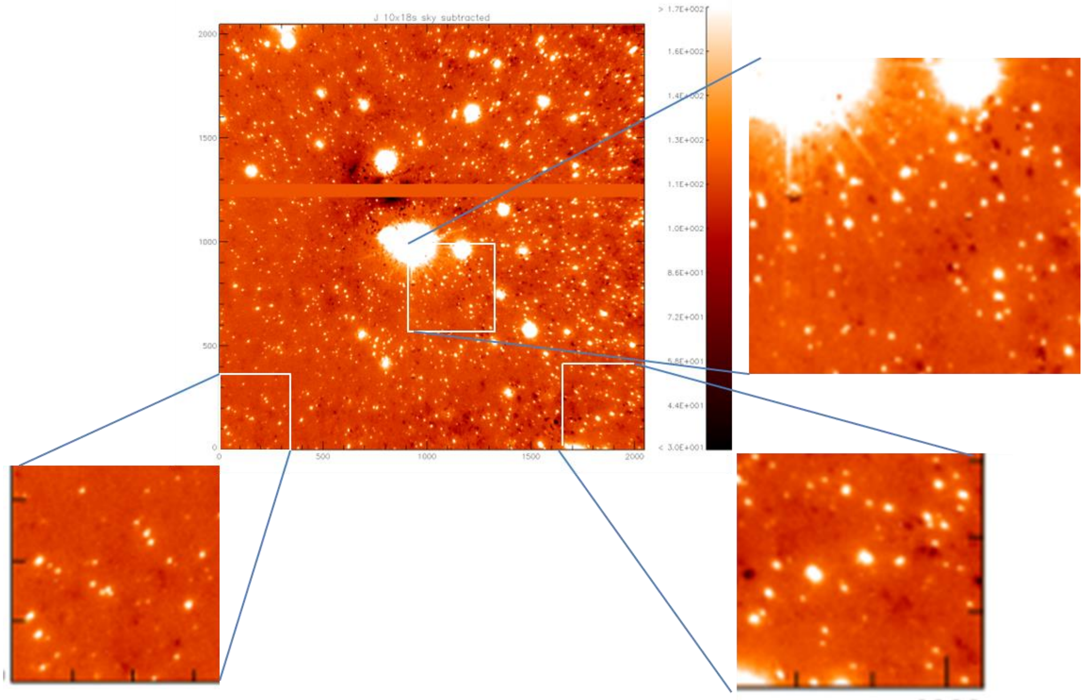

Figure 18. LUCI frames in J-band obtained with 3min exposure and sky self-subtracted. The AO reference star is at the brightest one at the center of the frame.

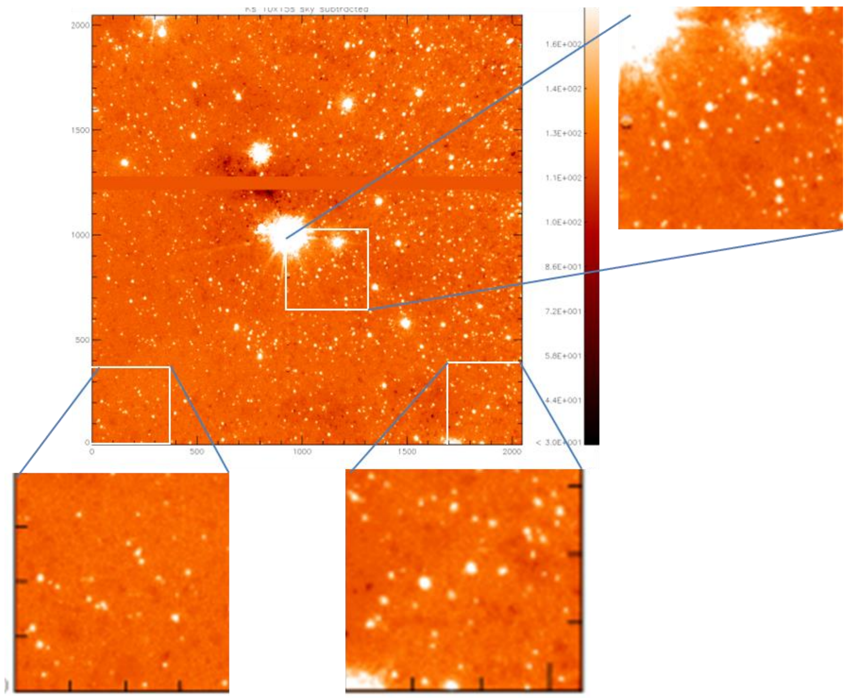

Figure 19. LUCI frames in Ks-band obtained with 3min exposure and sky self-subtracted. The AO reference star is at the brightest one at the center of the frame.

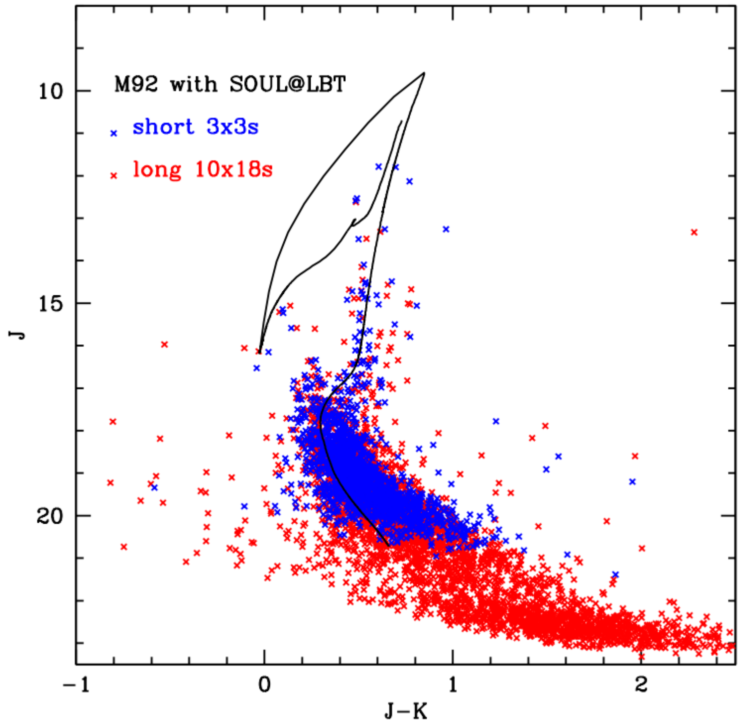

Figure 20. The CMDs in J, J-Ks (left) and Ks, J-Ks (right) obtained using both short (blue) and long (red) exposures data. The black solid line is an ad hoc isochrone from the BASTI website, see the text for details.

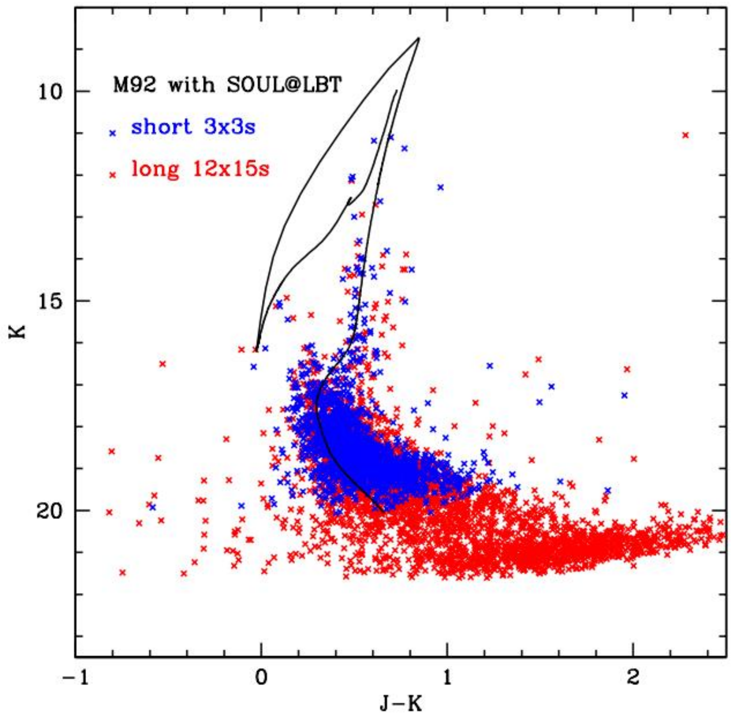

Figure 21. The CMDs in J, J-Ks (left) and Ks, J-Ks (right) obtained using both short (blue) and long (red) exposures data. The black solid line is an ad hoc isochrone from the BASTI website, see the text for details.

6.3 Extragalactic

6.3.1 AGN J1630+1649

This object is a candidate as multiple AGN. The integrated magnitude of the object is K17. The AO reference was placed at 27” far from the target. The central peak of AGN J1630 did not show evidence of multiplicity in this image. The field object on the left of Figure 22 shows a peak with FWHM of 90mas that can be considered as an upper limit for the achieved spatial resolution in this observation. The distance from the AO ref of the field object is 20” approximatively.

AO Parameters	Value
AO reference star	B 13.5 - V 13.0 - **R 13.0**
Distance from the target	27’’
Seeing (DIMM Line of sight)	0.6”-0.9” (03Jul2020)
# of corrected modes	250
AO loop frequency	800 Hz
WFS binning	2x2 (20x20SA)

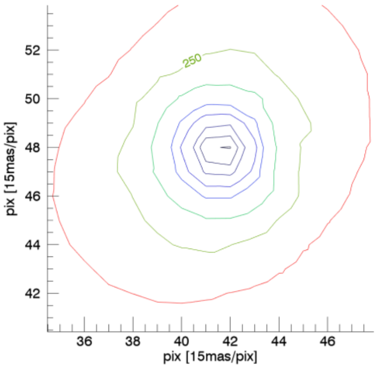

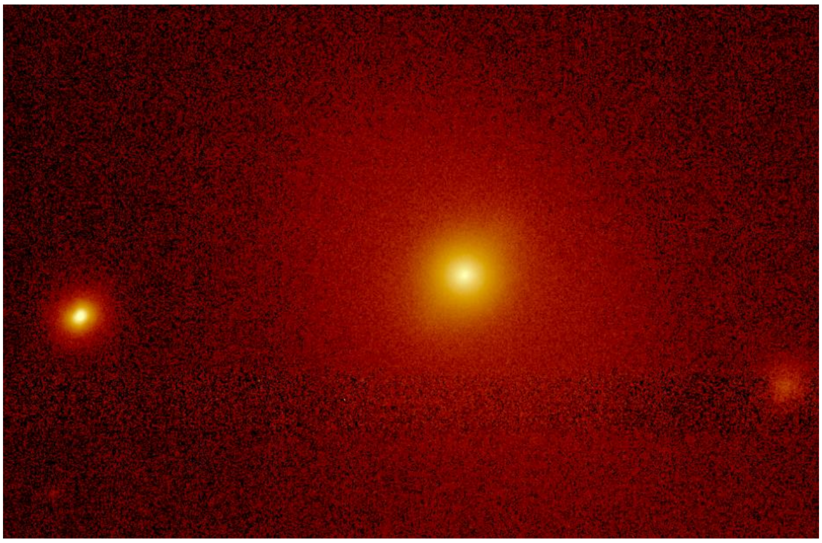

Figure 22. *Right*: frame obtained with a total of 960s on target and 480s off target for sky subtraction. AGN J1630+1649 is the object in the center of the frame at its left a field object. *Left*: contour plot of the field object showing a round peak of FHWM of 90mas.

6.3.2 Morphology of distant galaxies

SOUL+LUCI1 observed two galaxies part of an over density of objects around J1030, a Compton-thick FRII radio galaxy at z~1.7. Most of the overdensity members are blue, compact galaxies that are actively forming stars at rates of ~8–60 M⨀ yr−1. Ks-band imaging allowed to measure half-light radii of 2.2 ± 0.8

kpc at 8000 Å rest-frame for the brightest of them. The results are described in Gilli et al.[8]

The J1030 field was observed on 8 April 2019 during the SOUL commissioning. A bright NGS (R~ 12) close to the FRII radio galaxy allows for high-resolution AO observations. The field was observed for 40min in the *Ks* filter under seeing between 0.8′′ and 1.0′′, and the data were reduced with standard procedures. Although the reference star was found to be a double system with 0.4′′ of separation and a factor of ~4 in flux ratio, the AO correction provided a point spread function (PSF) down to FWHM = 72 × 76 mas at 23′′ of distance to the NGS on the single one-minute images. The final combined image has FWHM = 90 × 120 mas at the same distance.

AO Parameters	Value
AO reference star	**R12** (double!)
Distance from the target	23"
Seeing (DIMM Line of sight)	0.8-1.0" (09 Apr 2019)
# of corrected modes	250
AO loop frequency	1.0 kHz
WFS binning	2

Two galaxies (including the FRII radio galaxy) were detected and well spatially resolved. A full PSF deconvolution and morphological fitting was performed (see Figure 24) , but the final uncertainties on the Sersic index and half-light radius are large due to the limited S/N. Nevertheless, a reliable half-light radius r50 can be measured by aperture photometry, obtaining r50 = 0.26±0.1′′, corresponding to 2.2 ± 0.8 kpc at z ~1.7, for one galaxy, and r50 =0.27±0.05′′ (2.3±0.4kpc at z~1.7) for the radio galaxy.

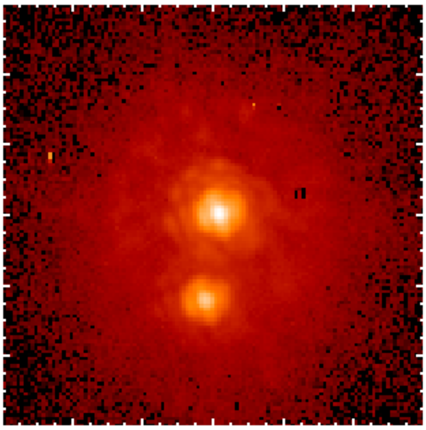

Figure 23. The AO reference star used for this observation is double with separation of about 0.4", as shown in this crop in H-band. This reduced the AO performance without compromising the scientific result.

[8] Gilli R. et al., "Discovery of a galaxy overdensity around a powerful, heavily obscured FRII radio galaxy at z = 1.7: star formation promoted by large-scale AGN feedback?", Astronomy and Astrophysics, vol. 632. 2019. doi: 10.1051/0004-6361/201936121...

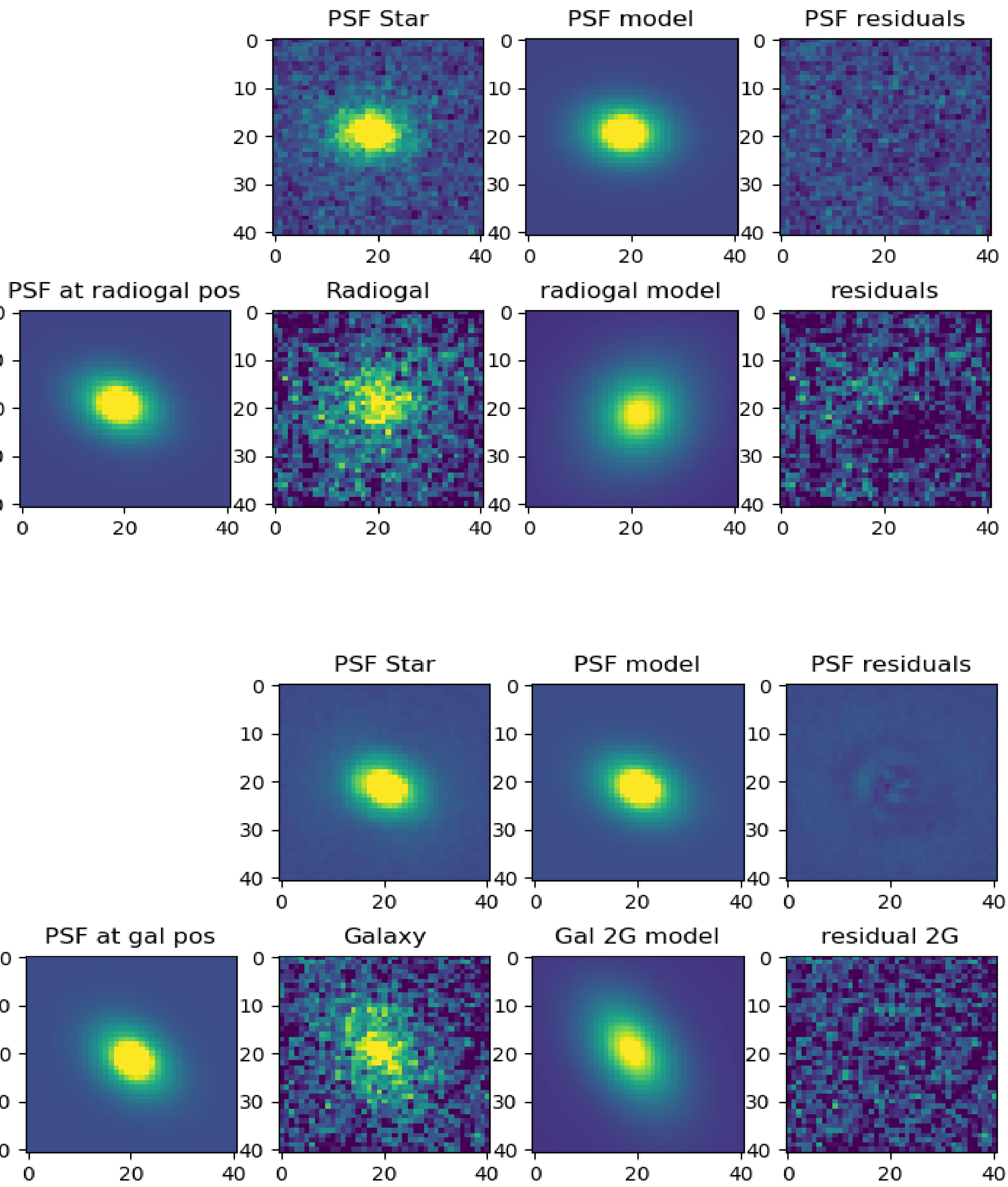

Figure 24. SOUL-LUCI1 imaging for the J1030 radiogalaxy (upper two lines) and for one galaxy of the associated overdensity at z~1.7. For each object we show the process of PSF deconvolution and morphological fitting.
For each object, the upper line show the field star used to measure the PSF, its modelling and the associated residuals.
The lower lines show the modeled PSF at the position of the target galaxy, the image of the galaxy, the best-fitting 2D model obtained by convolving a Sersic profile for the model PSF, and the residuals. Each panel is 0.6"x0.6", the scales are in pixels (15 mas/pixel).

6.3.3 Double star (fake extragalactic)

This is not an extragalactic object, but this result can be interesting for extragalactic observations, as some multiple AGN can be bright enough to be used as AO reference. This is a double star with components having similar magnitude and separated about **350mas**. These are critical conditions for wavefront sensing, but SOUL system has been able to provide a level of correction sufficient to provide round and well separated images of the two components.

AO Parameters	Value
AO reference star (integrated)	**R 15**
Distance from the target	0’’
Seeing (DIMM Line of sight)	1.0”
# of corrected modes	90
AO loop frequency	316 Hz
WFS binning	3x3 (13x13 SA)

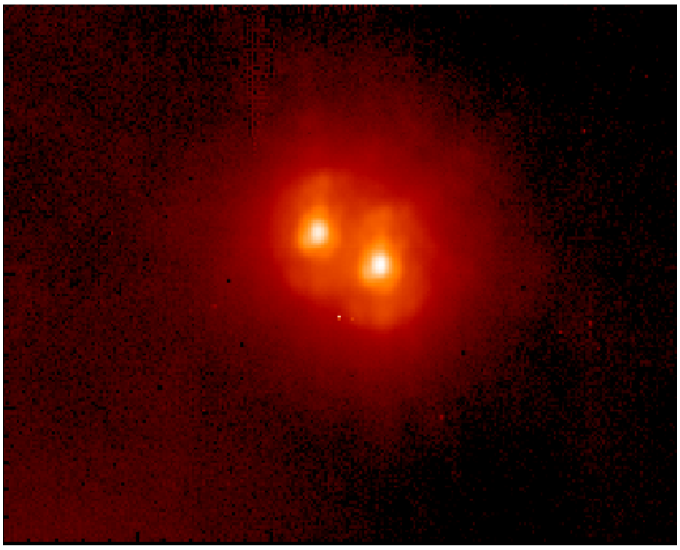

Figure 25. The double star used as AO reference, cropped frame with 3.75” side.

Appendix 1. WFS magnitude calibration

The WFS's spectral band is 600-890 nm, which approximately corresponds to the combination of R and I bands and the WFS magnitude is computed from a single reference flux. This means that when looking at different stellar types, the WFS magnitude can significantly change for a same given R magnitude. In order to understand the relation between the WFS magnitude, hereafter called RI magnitude, and the R magnitude, we plotted the difference RI-R as a function of the star color R-I (Figure 26).

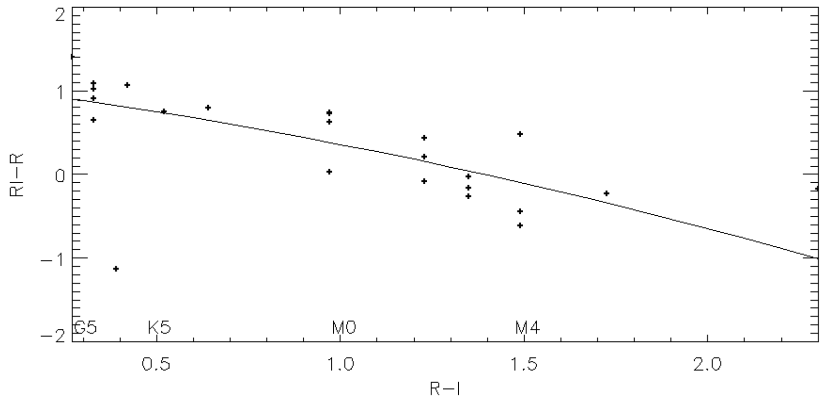

Figure 26. Difference between the WFS magnitude (RI) and the R magnitude from catalogs as a function of the R-I color. Solid line: fit from the analysis in this section. A few spectral types are indicated on their corresponding color on the X axis.

The difference RI-R tends to be 0 around the color R-I = 1.35, which corresponds to a M3 star, hence the reference flux has been defined with respect to a M3 star. We can then compute the ratio between the actual flux received from a given stellar type at R = 0 and the reference flux. This computation was made thanks to Pickles spectra and used to derive an analytical expression of RI-R as a function of the color R-I, that is the fit in Figure 26.

We are thus now able to predict the WFS magnitude as a function of the R magnitude and the spectral type (or equivalently the color R-I).